

# PCCP

Accepted Manuscript



This is an *Accepted Manuscript*, which has been through the Royal Society of Chemistry peer review process and has been accepted for publication.

*Accepted Manuscripts* are published online shortly after acceptance, before technical editing, formatting and proof reading. Using this free service, authors can make their results available to the community, in citable form, before we publish the edited article. We will replace this *Accepted Manuscript* with the edited and formatted *Advance Article* as soon as it is available.

You can find more information about *Accepted Manuscripts* in the [Information for Authors](#).

Please note that technical editing may introduce minor changes to the text and/or graphics, which may alter content. The journal's standard [Terms & Conditions](#) and the [Ethical guidelines](#) still apply. In no event shall the Royal Society of Chemistry be held responsible for any errors or omissions in this *Accepted Manuscript* or any consequences arising from the use of any information it contains.



PCCP

ARTICLE

## Exploring the nature of the liquid-liquid transition in silicon: A non-activated transformation†

Y. J. Lü,<sup>a,d\*</sup> X. X. Zhang,<sup>b</sup> M. Chen<sup>b</sup> and Jian-Zhong Jiang<sup>c,d</sup>

Received 00th January 20xx,  
Accepted 00th January 20xx

DOI: 10.1039/x0xx00000x

www.rsc.org/

In contrast to other glass formers, silicon exhibits a thermodynamic discontinuity between its liquid and amorphous solid states. Some researchers have conjectured that a first-order phase transition occurs between two forms of liquid silicon: the high-density liquid (HDL) and the low-density liquid (LDL). Despite the fact that several computer simulations have supported a liquid-liquid phase transition (LLPT) in silicon, recent work based on surface free energy calculations contradicts its existence and the authors of this work have argued that the proposed LLPT has been mistakenly interpreted [J. Chem. Phys. 138, 214504 (2013)]. A similar controversy has also arisen in the case of water because of discrepancies in the calculation of its free energy surface [Nature, 510, 385 (2014); J. Chem. Phys. 138, 214504 (2013)]. Current evidence supporting or not supporting LLPT is mostly derived from the thermodynamic stability of the LDL phase. Provided that the HDL-LDL transition is a first-order transition, the formation of LDL silicon should be an activated process. Following this idea, the nature of the LLPT should be clarified by tracing the kinetic path toward LDL silicon. In this work, we focus on the transformation process from the HDL to the LDL phase and use the mean first passage time (MFPT) method to examine thermodynamic and dynamic trajectories. The MFPT results show that the presumed HDL-LDL transition is not characterized by a thermodynamic activated process but by a continuous dynamic transformation. The LDL silicon is actually a mixture of the high-density liquid and a low-density tetrahedral network. We show that the five-membered Si-Si rings in the LDL network play a critical role in stabilizing the low-density network and suppressing the crystallization.

### 1. Introduction

The hypothesis of a liquid-liquid phase transition (LLPT) in silicon was initially proposed for interpreting the structural and thermodynamic gaps between the liquid and amorphous phases.<sup>1-6</sup> Liquid silicon is metallic at high temperatures and has a coordination number of approximately 7, whereas amorphous solid silicon exhibits semiconducting properties and has an open network structure with a coordination number of approximately 4. In addition, the extrapolated Gibbs free energies of the amorphous and liquid phases do not join smoothly.<sup>1</sup> These dissimilarities appear to be reasonably explained by the assumption that a phase transition occurs between two forms of liquid silicon: the low-density liquid (LDL) and the high-density liquid (HDL). Earlier molecular dynamics (MD) simulations showed that the transition from a

high-temperature liquid to a LDL is accompanied by a release of latent heat in the constant temperature and volume (NVT) and the constant enthalpy and pressure (NPH) ensembles, indicating a first-order thermodynamic transition.<sup>2,3</sup> Analogous to the LLPT in water, the LLPT in silicon is claimed to be terminated at a critical point.<sup>4</sup> In fact, whether a first-order LLPT in tetrahedral liquids occurs has long been a controversial issue. Chandler *et al.* calculated the free energy surfaces of several atomistic models including Stillinger-Weber (SW) silicon, monatomic water (mW) and ST2 water, and found that there is no one stable or metastable liquid phase basin in the supercooled region.<sup>7,8</sup> They argued that the LDL phase of ST2 water observed in previous computer simulations is an artifact associated with the non-equilibrium and finite-time sampling, and the LLPT is actually a coarsening of ice. This was then contradicted by Debenedetti *et al.*,<sup>9-11</sup> who presented two metastable liquid phases of ST2 water on the reversible free energy surface. Moreover, the transition between the two liquids has the characteristic feature of first-order phase transition, namely the LLPT does occur in ST2 water. Further studies on the possibility of an LLPT require new evidence from a different perspective on the process.

The HDL-LDL transition is initiated by nucleation in the LDL phase, provided that this process is a first-order thermodynamic transition; i.e., the existence of an LLPT is validated if the nucleation of LDL silicon is identified. Nucleation is a thermodynamically activated process in which

<sup>a</sup>School of Physics, Beijing Institute of Technology, Beijing 100081, P. R. China. E-mail: 04537@bit.edu.cn

<sup>b</sup>Department of Engineering Mechanics, Tsinghua University, Beijing 100084, P. R. China.

<sup>c</sup>International Center for New-Structured Materials (ICNSM), Zhejiang University and Laboratory of New-Structured Materials, School of Materials Science and Engineering, Zhejiang University, Hangzhou 310027, P. R. China

<sup>d</sup>State Key Laboratory of Silicon Materials, Zhejiang University, Hangzhou 310027, P. R. China.

†Electronic Supplementary Information (ESI) available: The calculated structure, thermodynamic, and dynamic properties of LDL silicon as well as the comparisons with the previous reported data. See DOI: 10.1039/x0xx00000x

the system crosses a free energy barrier into a new stable or metastable state. The kinetic trajectory of an activated process can be traced by the average time between when the system is activated to when it reaches the next state for the first time — the so-called mean first passage time (MFPT).<sup>12-14</sup> Prompted by this analysis, we here report our investigation of the presumed HDL-LDL transition using the MFPT method. We show that this transition is characterized by a continuous transformation associated with the maximum compressibility in both thermodynamics and dynamics. We provide a comprehensive structural description of LDL silicon and elucidate the critical role of five-membered covalent rings in the transformation.

## 2. Computation Methods

### 2.1 Molecular dynamics simulations

The present investigations were implemented using MD simulations. The Stillinger-Weber (SW) potential was adopted to calculate interatomic interactions.<sup>15</sup> In the SW potential, the total energy of a system was approximated by a combination of the two-body and the three-body contributions as follows,

$$E = \sum_i \sum_{j>i} \phi_2(r_{ij}) + \sum_i \sum_{j \neq i} \sum_{k>j} \phi_3(r_{ij}, r_{ik}, \theta_{ijk}) \quad (1)$$

$$\phi_2 = A\epsilon_{ij} \left[ B \left( \frac{\sigma_{ij}}{r_{ij}} \right)^p - \left( \frac{\sigma_{ij}}{r_{ij}} \right)^q \right] \exp \left( \frac{\sigma_{ij}}{r_{ij} - b\sigma_{ij}} \right)$$

$$\phi_3 = \lambda\epsilon_{ijk} \left( \cos\theta_{ijk} + \frac{1}{3} \right)^2 \exp \left( \frac{\gamma\sigma_{ij}}{r_{ij} - b\sigma_{ij}} \right) \exp \left( \frac{\gamma\sigma_{ik}}{r_{ik} - b\sigma_{ik}} \right)$$

where  $\phi_2$  and  $\phi_3$  are the two-body and the three-body terms, respectively.  $r_{ij}$  is the distance between atoms  $i$  and  $j$ , and  $\theta_{ijk}$  is the angle between vectors  $\mathbf{r}_i$  and  $\mathbf{r}_k$  subtended at the point  $j$ .  $\sigma_{ij}=2.0951$  Å and  $\epsilon_{ij}=2.0913$  kJmol<sup>-1</sup> for silicon, and the values of the parameters  $A$ ,  $B$ ,  $p$ ,  $q$ ,  $b$  and  $\lambda$  are referred to Ref. 15.

The supercooled HDL phase was first prepared by isobaric quenching in the NPT ensemble as the following procedure: The system was equilibrated at 2000 K for 2 ns, then cooled to 1300 K at a rate of 100 K per 1.2 ns, and finally cooled down to 1200 K at a rate of 10 K per 1.2 ns. The temperature and pressure were controlled with the Nosé and Hoover thermostat and barostat, respectively.<sup>16-18</sup> In addition, to test enthalpy-temperature behaviour at different pressures, we cooled the systems to 1300–1400 K in the NPT ensemble. The thermostat was then switched off, and the cooling was continued in the NPH ensemble while the sampling time remained 1.2 ns. Periodic boundary conditions were applied in all three directions. All the simulations were performed using the code LAMMPS<sup>19</sup> and a time step of 1 fs was used for integration.

### 2.2 Mean first passage time

The MFPT  $\tau(x)$  is defined as the average elapsed time that a system starting at the initial state  $x_0$  leaves a given domain for the first time. For a continuous transition process,  $\tau(x)$  shows a monotonic increase as the transition proceeds. If the process is activated, the MFPT

exhibits a sigmoidal shape, which distinguishes it from non-activated MFPTs.

Nucleation is an activated process characterized by overcoming the free energy barrier. The dynamics of the activated process can be described using a Fokker-Planck equation:<sup>20</sup>

$$\frac{\partial P(x,t)}{\partial t} = \frac{\partial}{\partial x} [D(x)e^{-\beta\Delta G(x)} \frac{\partial}{\partial x} (P(x,t)e^{\beta\Delta G(x)})] = -\frac{\partial J(x,t)}{\partial x}$$

where  $x$  is the reaction coordinate,  $P(x,t)$  is the probability density at  $x$  and time  $t$ ,  $D(x)$  is a generalised diffusion coefficient,  $J(x,t)$  is the state current,  $\Delta G(x)$  is the free energy barrier and  $\beta=1/k_bT$ . The steady-state rate of crossing the free energy barrier can be measured by the MFPT,  $\tau(x)$ . The MFPT for an activated process described in Eq. 2 is then given by<sup>21</sup>

$$\tau(x) = \int_{x_0}^x \frac{1}{D(y)} dy \exp[\beta\Delta G(y)] \int_a^y dz \exp[-\beta\Delta G(z)] \quad (3)$$

where  $a$  is the transition state corresponding to the top of the free energy barrier. The barrier crossing rate (nucleation rate in the case of crystallization) is related to the MFPT by<sup>21</sup>

$$J = \frac{1}{2\tau(x^*)} \quad (4)$$

where  $x^*$  is the reaction coordination corresponding to the transition state, which can be evaluated on the basis of the location of the inflection point in the MFPT curve. In our simulations, we adopted the alternative method that was proposed by Wedekind *et al.* to calculate the nucleation rate.<sup>12,13</sup> This method allows us to evaluate the critical size,  $x^*$  and the nucleation rate,  $J$  by fitting the MFPT to the following expression:

$$\tau(x) = \frac{\tau_J}{2} [1 + \operatorname{erf}((x - x^*)c)] \quad (5)$$

where  $\tau_J = 1/J$ ,  $\operatorname{erf}(x)$  is the error function, and

$$c = \sqrt{\frac{|\Delta G''(x^*)|}{2k_bT}} \quad (6)$$

For an activated process, when the system crosses the activated barrier and reaches a steady state, the probability density  $P_{st}(x)$  has the time independence,  $\partial P_{st}/\partial x = -\partial J/\partial x = 0$ , thus Eq. 2 is rewritten as

$$\frac{\partial(\beta\Delta G(x))}{\partial x} = -\frac{\partial \ln P_{st}(x)}{\partial x} - \frac{J}{D(x)P_{st}(x)} \quad (7)$$

The free energy barrier is then given by<sup>12,13</sup>

$$\beta\Delta G(x) = \ln[B(x)] - \int_a^x \frac{dx'}{B(x')} + C \quad (8)$$

where

$$B(x) = \frac{1}{P_{st}(x)} \left[ \int_0^x P_{st}(x') dx' - JV\tau(x) \right] \quad (9)$$

and  $V$  is the system volume. Using Eqs. 8 and 9,  $\Delta G(x)$  can be calculated from the knowledge of  $P(x,t)$ ,  $J$  and  $\tau(x)$ . Then, the nucleation barrier,  $\Delta G(n^*)$  is obtained from the maximum of  $\Delta G(x)$ .

In the simulations, the reaction coordinate was the size of the largest LDL or crystalline cluster. The cluster was identified using three kinds of order parameters associated with the volume, locally structural order and dynamic activity, respectively. We calculated the MFPT for the HDL-LDL transition at  $T = 1060$  K,  $P = 0$  GPa and that for crystallization at  $T = 1080$  K,  $P = 0$  GPa. The initial configurations were selected from the quenched HDL systems at 1200 K. In each simulation, the size of the largest cluster was calculated at regular intervals (2–20 ps depending on the choice of the order parameter), and the time at which it appears for the first time was stored. The MFPT  $\tau(n)$  was then obtained by averaging several trajectories. Each trajectory sampling was run for 10 ns ( $10^7$  MD steps) and a total of 200 independent samplings were performed from a set of initial configurations with newly randomized velocities. The system-size dependence of MFPT was examined for  $N = 1000$ , 2744 and 4096.

### 2.3 Local order structure

In the structural analyses, we employed three local order parameters: the local structure index (LSI),  $I$ , the local bond-orientational order parameter,  $q$ , and the structural order parameter,  $a$ , based on the CHILL algorithm, respectively. The LSI was used to measure the inhomogeneity of atoms distributed in the coordination shells.<sup>22</sup> The LSI,  $I(o,t)$  of the atom  $o$  at time  $t$ , is defined as

$$I(o,t) = \frac{1}{n} \sum_{i=1}^n [\Delta(i;o,t) - \bar{\Delta}(o,t)]^2 \quad (10)$$

where  $\Delta(i;o,t) = r_{i+1} - r_i$  and  $r_i$  is the distance between atom  $o$  and its  $i$ th neighbour. The atoms centered around atom  $o$  are sequenced according to distance:  $r_1 < r_2 < \dots < r_i < r_{i+1} < \dots < r_n < r_{n+1}$ , where  $n$  is chosen such that  $r_n < 3.2 \text{ \AA} < r_{n+1}$ .  $\bar{\Delta}(o,t)$  is the average of  $\Delta(i;o,t)$ ,  $\bar{\Delta}(o,t) = \sum \Delta(i;o,t) / n$ . The atoms with  $I > 0.08 \text{ \AA}^2$  are the locally ordered atoms, and those with  $I < 0.08 \text{ \AA}^2$  are locally disordered.

The local bond-orientational order parameter  $q$  is defined by

$$q(k) = 1 - \frac{3}{8} \sum_{i=1}^3 \sum_{j=i+1}^4 \left( \cos \theta_{ikj} + \frac{1}{3} \right)^2 \quad (11)$$

where  $\theta_{ikj}$  is the angle connecting atom  $k$  with two of its four closest neighbors,  $i$  and  $j$ ;  $q(k)$  is 1 for a tetrahedral configuration. For tetrahedral crystals and disordered liquids,  $q(k)$  shows different characteristic probability distributions, thereby allowing these structures to be identified.

First proposed by Moore and Molinero,<sup>23</sup> the CHILL algorithm is used to analyze the arrangement of adjacent tetrahedral configurations. In the algorithm, a local order parameter  $a(i,j)$  is defined by

$$a(i,j) = \frac{q_i(i) \cdot q_i(j)}{|q_i(i)| |q_i(j)|} \quad (12)$$

where

$$q_i(i) = \sum_{m=-l}^l q_{lm}(i), \quad (13)$$

$$q_{lm}(i) = \frac{1}{4} \sum_{j=1}^4 Y_{l,m}(\mathbf{r}_{ij}), \quad (14)$$

and  $\mathbf{r}_{ij}$  is a vector connecting the atom  $i$  with one of its four closest atoms  $j$ ;  $Y_{lm}(\mathbf{r}_{ij})$  are the spherical harmonics; and  $a(i,j)$  represents the alignment of the orientation between atom  $i$  and its closest neighbour,  $j$ . As  $l = 3$ ,  $a(i,j) = -1$  for a staggered bond and  $a(i,j) = -0.11$  for an eclipsed bond. In the simulations, the ensemble average of  $a(i,j)$  has a statistical distribution because of thermal fluctuations. We identified a staggered bond when  $a(i,j) < -0.8$  and an eclipsed bond when  $-0.2 < a(i,j) < -0.05$ .

We used the three vertex ring count algorithm to count the polygons composed of Si-Si covalent bonds, where only the smallest rings with continuous Si-Si bonding were considered.<sup>24</sup>

## 3. Results and Discussion

### 3.1 Non-thermodynamic transition

Crystallization starts from an activation-type nucleation followed by continuous crystal growth. Because the time scale for crystal growth is much smaller than that for nucleation, the MFPT curve ultimately reaches a plateau after a sharp rise, displaying a sigmoidal shape. The MFPT curve provides us a straightforward method to check whether a transition is initiated from nucleation. If the LLPT is a first-order transition, the MFPT curve should exhibit a sigmoidal-type increase corresponding to the nucleation of the LDL phase. Prior to verifying this, we need to choose appropriate order parameters to distinguish the LDL from the HDL environment. Given the considerable changes in density, locally structural order and dynamic slowdown through the HDL-LDL transition,<sup>3,4</sup> we chose three independent order parameters associated with density, structure and dynamics to trace the HDL-LDL path in parallel. The first one is LSI,  $I$ , which quantifies locally tetrahedral order within the first and second coordination shells. The second one is the atomic volume. An attempt to clearly identify LDL silicon using the Voronoi atomic volume<sup>25</sup> failed. Instead, we define an average atomic volume,  $l$ ,

$$l_i = \left[ \frac{1}{N_a + 1} \sum_{i=0}^{N_a} v_i^2 \right]^{\frac{1}{2}} \quad (15)$$

where  $v_i$  is the Voronoi volume of atom  $i$ ,  $N_a$  is the nearest-neighbouring coordination number, and  $i = 0$  denotes atom  $i$  itself. This index holds the information of the atomic volume in both the first and the second coordination shells, and thus improves the identification of large-volume atoms. (see Fig. S1 of the ESI†) The last one is the local dynamic activity,  $k_i$ ,

$$k_i = \sum_{t=0}^{t_{\text{obs}}} |r_i(t + \Delta t) - r_i(t)|^2, \quad (16)$$

where  $r_i(t)$  is the atom position at time  $t$ ;  $k_i$  sums the squared displacement of atoms  $i$  between  $t$  and  $t + \Delta t$  over the observation period,  $t_{\text{obs}}$ , and along the trajectory to another state. The incremental time,  $\Delta t$ , is taken as the time interval in which atoms in normal liquid silicon move a diameter distance. This order parameter has shown a good performance in the studies of dynamic glass transition.<sup>26</sup> The volume-, structure- and dynamics-based MFPTs (i.e.,  $l$ -,  $I$ - and  $k$ -MFPT) for SW silicon were calculated using MD simulations in the isothermal-isobaric (NPT) ensemble, respectively. A trial was first made for the crystallization of diamond-structured silicon (Si-I) in HDL at 1080 K and  $N=2744$ , as shown in Fig. 1a. All the MFPTs indicate that the crystallization of Si-I is an activated process. Although the critical nucleus sizes evaluated from the inflection points of MFPT curves differ from each other, the nucleation rates that are inversely proportional to the nucleation time,  $\tau$ , are approximately identical. Then, we used the three order parameters to trace the HDL-LDL transition. Before the MFPT calculations, we first estimated the LLPT temperature by quenching the system from  $T = 1200$  K. The rapid decrease of density suggests the existence of a low-density phase below 1060 K at zero pressure. The structural

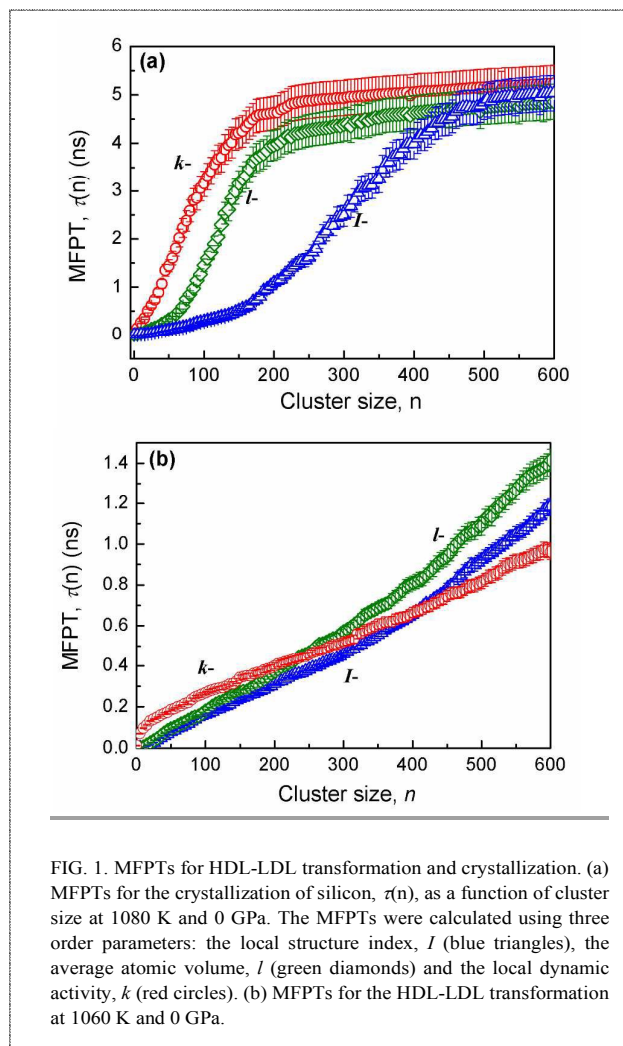


FIG. 1. MFPTs for HDL-LDL transformation and crystallization. (a) MFPTs for the crystallization of silicon,  $\tau(n)$ , as a function of cluster size at 1080 K and 0 GPa. The MFPTs were calculated using three order parameters: the local structure index,  $I$  (blue triangles), the average atomic volume,  $l$  (green diamonds) and the local dynamic activity,  $k$  (red circles). (b) MFPTs for the HDL-LDL transformation at 1060 K and 0 GPa.

and thermodynamic characteristics of this low-density silicon have been proven to be identical to those of reported LDL silicon. (see ESI†) Therefore, we speculate that LLPT occurs around  $T=1060$  K. The growth trajectory of LDL clusters was sampled at 1060 K and zero pressure, and a total of 200 independent trajectories were averaged to obtain the MFPTs (i.e.,  $l$ -,  $I$ - and  $k$ -MFPT) of the HDL-LDL transition. Figure 1b illustrates the  $l$ -,  $I$ - and  $k$ -MFPTs as a function of largest cluster size for the HDL-LDL transition. All of three MFPTs do not exhibit the sigmoidal growth like an activated process; the clusters continuously grow without any evidence of overcoming a free energy barrier. The presumed LLPT in silicon is actually not a first-order transition in thermodynamics.

Generically, the crystallization proceeds in two manners.<sup>27</sup> If there is nucleation characterized by a free energy barrier that must be overcome, the crystallization shows an activated process, for example, the crystallization of Si-I phase shown in Fig. 1a. In this manner, there is an introduction period before nucleation. The second manner is the coarsening of crystalline nuclei in which numerous subcritical nuclei disperse in supercooled liquids and the growth of nuclei undergoes through the aggregation between them. In the process, the introduction period is not well distinguished. For the nucleation-dominated crystallization, the crystallization time depends on the system size;<sup>27</sup> in contrast, for the coarsening process, such dependence becomes much weak. We calculated the nucleation rate in unit volume,  $J_V=J/V$  by fitting the MFPTs to Eq. 5 and then the free energy barriers of crystallization from Eqs. 8 and 9 for  $N=1000$ , 2744 and 4096. Despite that the values of the free energy barriers decrease from 3.89 to 1.70  $k_B T$  with increasing system size,  $J_V$  actually decreases, as shown in Fig. 2, implying that the number of the critical nucleus per unit time and volume decreases and correspondingly the mean crystallization time increases. We traced the crystallization processes as a function of time for the three systems using  $k$  parameter, and Figure 3a presents the corresponding growth curves of crystalline Si. The inset in Fig. 3a shows that the crystallization time that is approximately determined by the rise interval increases when the system size increases, which agrees with the speculation from the nucleation barriers. We then plotted the LLPT as a function of time, as shown in Fig. 3b. The LDL clusters form immediately when the systems relax at 1060 K, and then continuously grow without the introduction period. Furthermore, the growth rate does not depend on the system size: the three systems finish the transition nearly at the same time. These results clearly indicate that the HDL-LDL transformation in Si is a continuous dynamic slowdown rather than a first-order phase transition. This is consistent with the free energy calculations presented in Ref. 8. In contrast, however, freezing occurs by an activated process that is consistent with classical nucleation. Consequently, the appearance of the transient LDL phase cannot be attributed to the coarsening of crystalline phase as previously suggested.<sup>7,8</sup> Another problem of concern is whether the continuous transition results from the first-order-like LLPT close to the spinodal decomposition. Sastry *et al.* claimed that the liquid-liquid critical point of the SW silicon lies at  $T_c = 1120 \pm 12$  K,  $P_c = -0.60 \pm 0.15$  GPa.<sup>3</sup> To test its possibility, we sampled the LLPT at  $P = 1.2$  GPa, which is away from the estimated critical point. The transformation from HDL to the LDL silicon occurs at  $900 \pm 20$  K at  $P = 1.2$  GPa and proceeds by a continuous growth of LDL silicon like the case at  $P = 0$  GPa. Therefore, it is

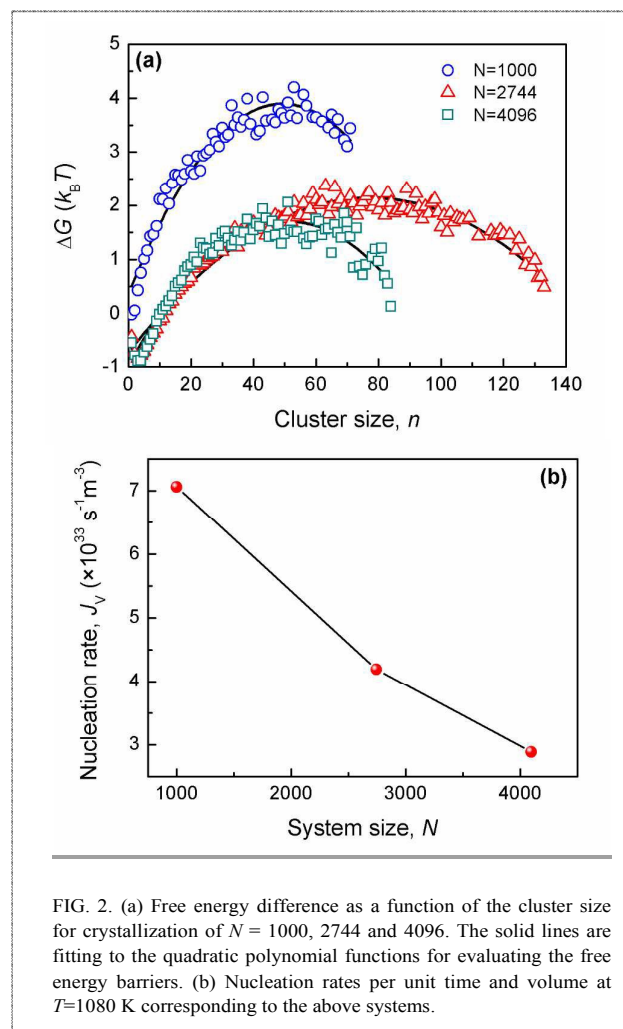


FIG. 2. (a) Free energy difference as a function of the cluster size for crystallization of  $N = 1000$ , 2744 and 4096. The solid lines are fitting to the quadratic polynomial functions for evaluating the free energy barriers. (b) Nucleation rates per unit time and volume at  $T=1080$  K corresponding to the above systems.

reasonable to exclude the possibility that the continuous transformation is due to the proximity to the spinodal.

Figure 4 shows the number of the LDL cluster as a function of simulation time at  $T = 1060$  K. The LDL cluster that is identified using the  $k$  parameter sharply increases during the first 0.25 ns and then slowly decreases by the end of simulations, suggesting that the transformation is dominated by the coalescence of clusters. For the nucleation-dominated crystallization, due to the growth of crystalline nuclei, the nucleus number exhibits a stable period until approaching the end of crystallization where the large crystalline clusters merged together. It is noteworthy that a weak plateau period ( $\Delta t = 0.34$  ns) appears in the HDL-LDL transformation for the system with  $N = 4096$ . It suggests that the LDL clusters also undergo a growth process, in other words, the LDL clusters tend to slow down the regions surrounding them, which likes the dynamic heterogeneity in the glassy system.<sup>28</sup> We speculate that this phenomenon becomes more distinct in the larger systems. The transformation processes measured by the density and structural ordering parameters,  $l$  and  $I$  exhibit the similar characteristics that are consistent with a dynamic transformation, rather than thermodynamic phase transition. Chandler *et al.* calculated the reversible free energy surfaces of supercooled mW water and SW silicon, in which they did not

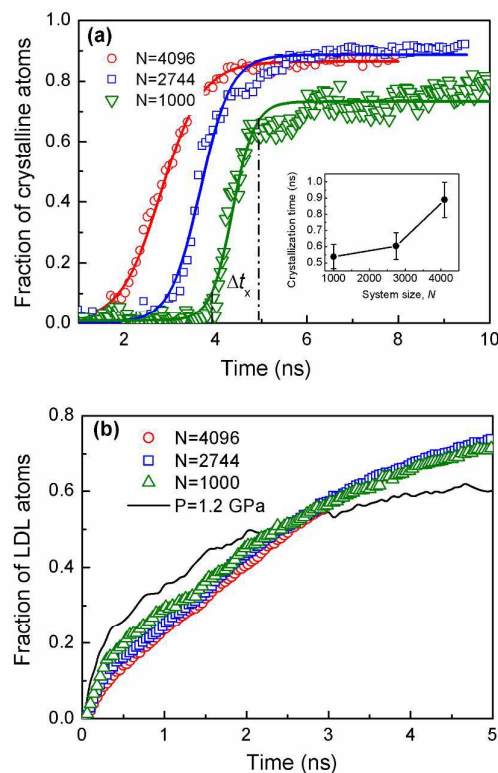


FIG. 3. (a) Fraction of crystalline atoms as a function of simulation time during crystallization. The green triangles, blue squares and red circles denote the cases of  $N = 1000$ , 2744 and 4096. The inset shows the crystallization time,  $\Delta t_x$  versus system size. (b) Fraction of LDL atoms as a function of simulation time in the HDL-LDL transformation. The solid curve shows the case at  $P = 1.2$  GPa for  $N = 2744$ .

observe the existence of a stable or metastable liquid phase.<sup>7,8</sup> Our observation qualitatively agrees with these free energy calculations.

Sciortino and co-workers showed that the softness of the intermolecular interactions and the flexibility of the bonds promote the LLPT in tetrahedral liquids.<sup>29</sup> They compared the softness and the flexibility of ST2, TIP4P and mW water and the SW silicon, and found that ST2 and TIP4P water have high flexibility due to the formation of hydrogen bonds.<sup>30</sup> It suggests that the LLPT is possible in ST2 and TIP4P water, which was supported by the subsequent numerical studies.<sup>31,32</sup> In contrast, the mW model is an atomistic model of water and it shows limited flexibility,<sup>30</sup> which reasonably interprets the simulation results that the LLPT is not achieved using the mW model.<sup>33</sup> Similar to the mW water, the three-body potential in the SW model induces a lack of bond flexibility. It is consistent with our conclusion that the LLPT is actually difficult to occur in the SW silicon.

### 3.2 Structure of LDL silicon

The LDL cluster has the characteristic of the locally tetrahedral order in the first and second coordination shells.<sup>3</sup> Consequently, the knowledge of the orientation relationship between the neighbouring tetrahedrons is necessary for an accurate description of the LDL structure. Tetrahedral crystals exhibit two geometric conformations:

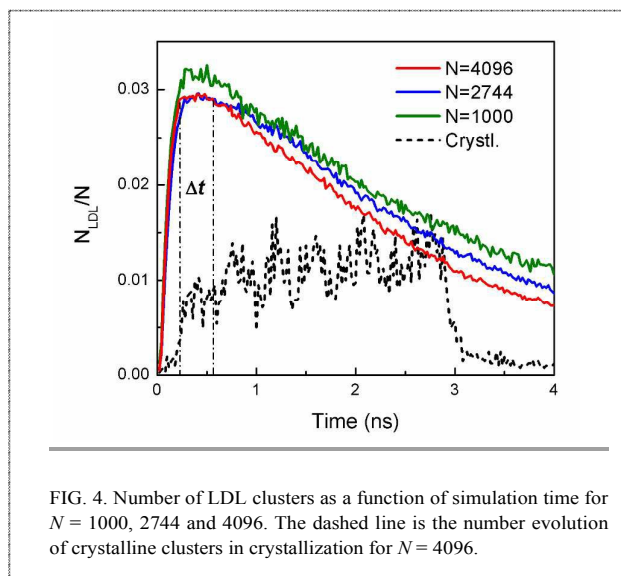


FIG. 4. Number of LDL clusters as a function of simulation time for  $N = 1000$ , 2744 and 4096. The dashed line is the number evolution of crystalline clusters in crystallization for  $N = 4096$ .

staggered and eclipsed. In the cubic phase, an atom bonds to its four closest neighbours in a staggered arrangement; in the clathrate phase, the four bonds are eclipsed. If the four bonds consist of three staggered bonds and one eclipsed bond, the atom belongs to the hexagonal phase. Aside from these arrangements, some arrangements exhibit partial characteristics of crystals; for instance, when the four bonds are only composed of two or three staggered bonds but at least one neighbour has more than two staggered bonds, they are defined as the interfacial phase by Moore *et al.*<sup>23</sup> The structural analyses using the local orientational order parameter,  $q$ , show that the largest low-density clusters are composed of two types of atoms with different local structures: more than 60% of the atoms are tetrahedral order, which is referred to as the LDL network, and

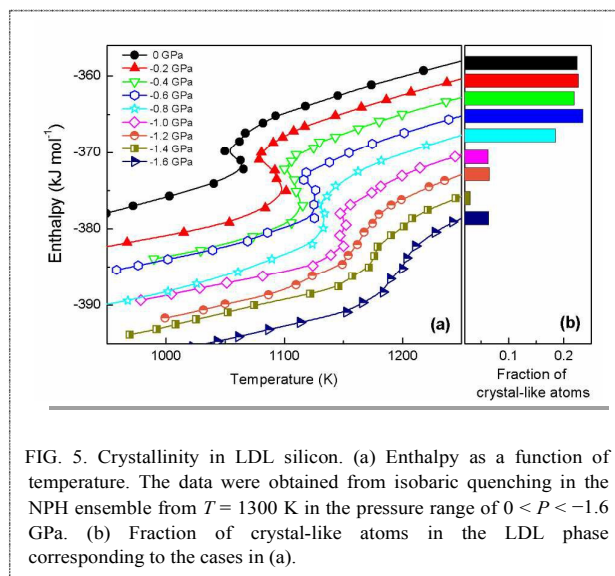


FIG. 5. Crystallinity in LDL silicon. (a) Enthalpy as a function of temperature. The data were obtained from isobaric quenching in the NPH ensemble from  $T = 1300$  K in the pressure range of  $0 < P < -1.6$  GPa. (b) Fraction of crystal-like atoms in the LDL phase corresponding to the cases in (a).

the remaining over 30% coordinate these tetrahedral atoms. In the LDL network, 55% of the atoms are arranged in random tetrahedral stacking and the remaining atoms are in crystalline (whose size reaches  $6 \pm 3\%$  of the whole system) and interfacial phase. The crystalline fragments remaining in the low-density phase have been extensively observed in experiments and simulations.<sup>33,34</sup> For example, the calorimetry and x-ray diffraction experiments have detected 5% ice in low-density amorphous (LDA),<sup>35</sup> which is in agreement with our results in LDL. The formation of crystallites is critical to understanding why the enthalpy-temperature curve displays a non-monotonic behaviour, which was taken as vital evidence for the existence of an LLPT in previous NPH and NVT simulations.<sup>3,5,6</sup> We quenched the liquid silicon to 1300 K using the

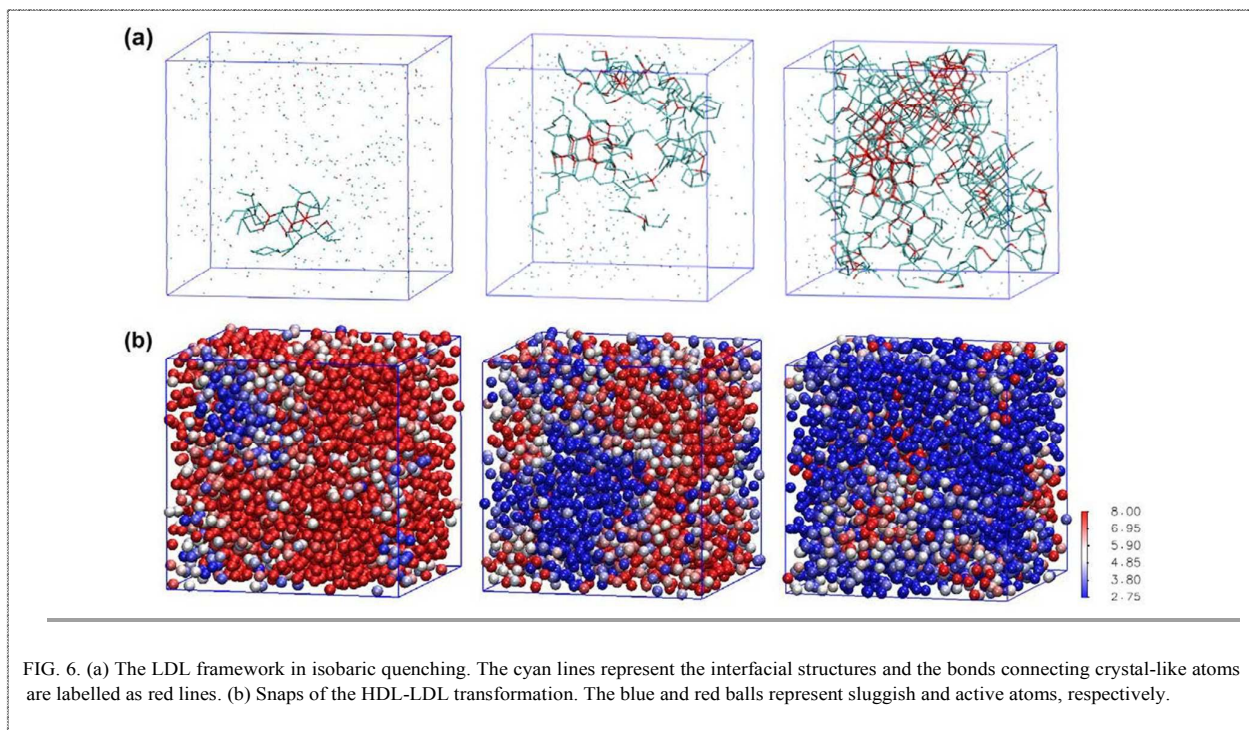


FIG. 6. (a) The LDL framework in isobaric quenching. The cyan lines represent the interfacial structures and the bonds connecting crystal-like atoms are labelled as red lines. (b) Snaps of the HDL-LDL transformation. The blue and red balls represent sluggish and active atoms, respectively.

NPT simulations and then continued to cool it in the NPH ensemble. The isobaric quenching covers a pressure range from 0 to  $-1.6$  GPa. Figure 5a shows that the enthalpy-temperature curves return to high-temperature values because of the release of latent heat during the transformation. The average intensity of the latent heat decreases with increasing tensile stress until it evolves into an inflection point at  $P = -1.0$  GPa and eventually disappears when  $P \leq -1.2$  GPa. We find that the pressure at which the latent-heat peaks are smoothed is consistent with the pressure at the liquid-liquid critical point estimated by first-principles calculations.<sup>5</sup> Figure 5b shows the fractions of crystal-like atoms in systems after the transformations; the temperature jumps due to the release of latent heat,  $\Delta T$ , are approximately linearly proportional to these fractions,  $f_x$ , as  $\Delta T \sim 74.8 f_x$ . We speculate that the latent heat is likely induced by the liquid-crystal transition rather than by what is known as liquid-liquid transition. When the tensile stress increases to greater than  $1.2$  GPa, the fraction is approximately 6% and the average radius of the crystallite is approximately  $1$  nm given a spherical shape. These crystallites are too small to be detected in the enthalpy-temperature curve and are therefore often mistakenly thought to result from the presence of a liquid-liquid critical point.

We note that the fractions of the crystal-like atoms in some NPH simulations reach 20% and the size of crystalline clusters exceeds that of the critical nuclei. However, the overall crystallization does not occur. Our task is now to account for why these crystalline clusters cannot stimulate further crystallization. The fraction of interfacial Si atoms remains at approximately 30% after a prolonged equilibration period. We refer to the tetrahedral network composed of crystalline and interfacial Si atoms as the “ordered LDL framework”, which is the intrinsic structure characterized by locally tetrahedral order. Figure 6a shows the evolution of the ordered LDL framework during the transformation. Small tetrahedral clusters form in the initial period and then consolidate into a three-dimensional configuration with a fractal dimension of  $2.6$  ( $P = 0$

GPa), (see Fig. S7 of the ESI†) where numerous five- and six-membered Si-Si covalent rings form. The ordered LDL framework greatly contributes to the slow dynamics of LDL Si, and its size is approximately 30% of the total slow atoms. More than one-third of the other slow atoms neighbour the ordered LDL framework in the first shell, and the remainder lie in the second neighbouring shell. Figure 6b shows snapshots of the system undergoing the dynamic HDL-LDL transition. The ordered LDL framework is the core of the slow region and it tends to slow down its neighbours in the medium range. Although several simulations have shown that the crystallization of Si preferentially occurs in the LDL region,<sup>36,37</sup> our work suggests that the catalytic effect of LDL on crystallization due to their similarity in structure will be countered by the low mobility of LDL. We compared the atomic mobility of the five-membered rings in the ordered LDL framework with that of the regular six-membered rings in the Si-I phase. From the results of the average  $k$  of atoms in the two types shown in Fig. 7a, the five-membered rings are more mobile than the regular six-membered rings, and both are much slower than the random five-membered rings in the high-density region (Fig. 7b). We find that the crystallites in LDL are usually surrounded by the LDL framework, particularly by the five-membered rings. It indicates that the growth of these crystallites requires the five-membered rings to be broken and the regular six-membered rings to be built up. Under the condition of high cooling rate, the systems do not sufficiently relax to break the five-membered rings, and consequently the growth of the crystallites is suppressed. Figure 7c provides a comparison between the fraction change of five-membered rings in the HDL-LDL transformation and that in crystallization. The number of five-membered rings begins to decrease at the onset of crystallization, whereas it continuously increases throughout the HDL-LDL transformation, which gives a direct evidence for our interpretation. The crystallites surviving in the LDL network serve as underlying growth sites to promptly trigger crystallization if the appropriate conditions are provided. For

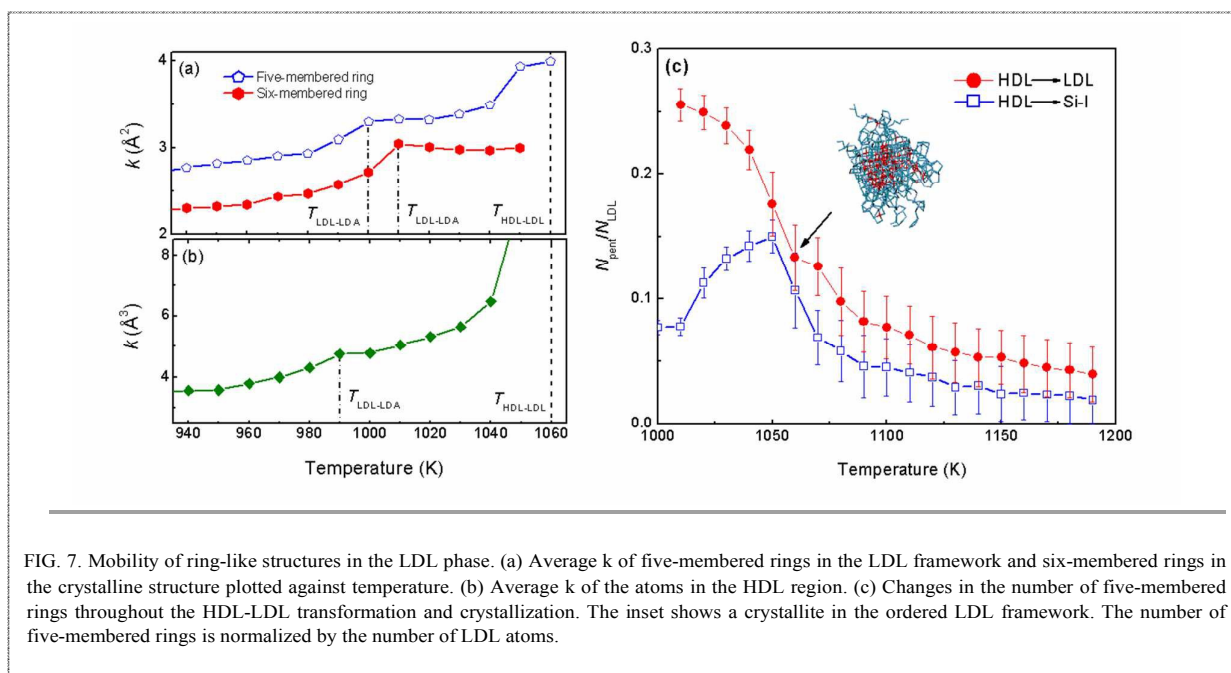


FIG. 7. Mobility of ring-like structures in the LDL phase. (a) Average  $k$  of five-membered rings in the LDL framework and six-membered rings in the crystalline structure plotted against temperature. (b) Average  $k$  of the atoms in the HDL region. (c) Changes in the number of five-membered rings throughout the HDL-LDL transformation and crystallization. The inset shows a crystallite in the ordered LDL framework. The number of five-membered rings is normalized by the number of LDL atoms.

example, we heated LDL silicon and observed that crystallization occurred exclusively. A reversible path from LDL to HDL was not achieved at the conditions investigated here. In addition, Figs. 7a and 7b show that the LDL phase undergoes another dynamic transition at  $T = 1000 \pm 10$  K, which should correspond to the transformation from LDL to LDA silicon. Although the LDL-LDA transition has been argued to proceed smoothly in thermodynamics,<sup>38</sup> we here show that it can still be identified by a dynamic signature.

The HDL-LDL transformation characterized by rapid but continuous changes in thermodynamic and dynamic properties is essentially a limited relaxation process in which tetrahedral atoms are clustered together to form a locally tetrahedral order framework. We calculated the isothermal compressibility,  $\kappa_T = -(\partial V/\partial P)_T/V$ , by decompressing liquid silicon from  $P = 5$  GPa to  $P = -4$  GPa at a rate of 0.2 GPa per 1.2 ns in the NPT ensemble, as shown in Fig. 8. The decompressing is terminated by liquid cavitation beyond  $-4.2$  GPa. In addition, the maximum density of liquid silicon is determined in the isobaric quenching simulations from  $T = 1800$  K to  $T = 900$  K at a rate of 20 K per 1.2 ns. Along the isothermal HDL-LDL path, the compressibility is shown to peak at the transformation temperature. The HDL-LDL transformation is simply a relaxation process.

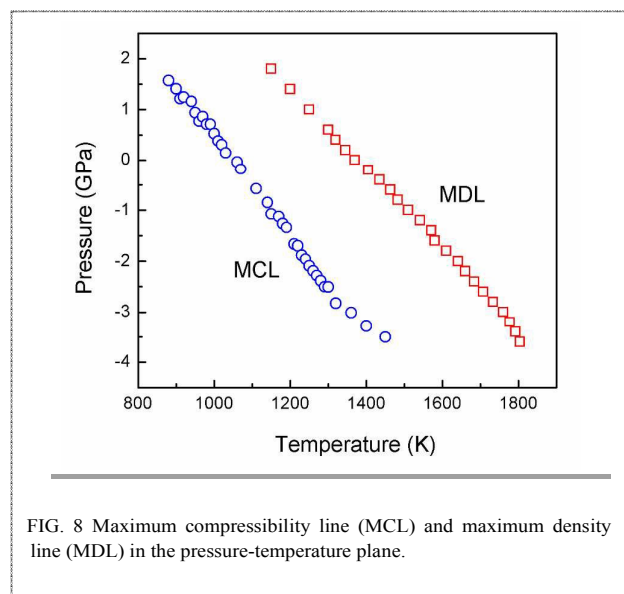


FIG. 8 Maximum compressibility line (MCL) and maximum density line (MDL) in the pressure-temperature plane.

#### 4. Conclusions

We investigated the kinetic trajectories of the HDL-LDL transformation in SW silicon using the MFPT method. The MFPTs based on the local structure, density and dynamic activity consistently show that the formation of LDL silicon does not follow the sigmoidal manner, which indicates that the putative LLPT in silicon is not a thermodynamic phase transition. In the HDL-LDL transformation, a large amount of LDL clusters form at the beginning of the simulation and then they continuously grow accompanied by the decrease of cluster number. Furthermore, we studied the system size dependence of the crystallization and HDL-LDL transformation, and found that the nucleation time increases considerably with increasing

system size, whereas the characteristic time for the HDL-LDL transformation less depends on the system size. All of the results suggest that the HDL-LDL transformation is a dynamic process. The LDL silicon is a precursor to amorphous solid silicon, or in a sense, the liquid counterpart of the amorphous phase.<sup>39</sup> We examined the non-monotonic behaviour of the enthalpy-temperature curves in the NPH simulations and confirmed that the liquid-crystal transition hidden in the HDL-LDL transformation is responsible for this phenomenon. Our simulations show that the dynamic process corresponds to the relaxation of the LDL framework associated with the maximum of compressibility. The five-membered Si-Si rings in the LDL framework are of importance in stabilizing the LDL framework and suppressing the crystallization.

#### Acknowledgements

Financial support from the National Basic Research Program of China (2012CB825700), the National Natural Science Foundation of China (51171027, 51371157 and U1432105), and the Fundamental Research Funds for the Central Universities are gratefully acknowledged. We thank the Shanghai and Tianjin Supercomputer Center for providing computing resources.

#### Notes and references

- 1 L. I. Aptekar, Phase transitions in noncrystalline germanium and silicon, *Sov. Phys. Dokl.*, 1979, **24**, 993-995.
- 2 P. H. Poole, T. Grande, C. A. Angell, and P. F. McMillan, Polymorphic Phase Transitions in Liquids and Glasses, *Science*, 1997, **275**, 322-323.
- 3 S. Sastry and C. A. Angell, Liquid-liquid phase transition in supercooled silicon, *Nature Mater.*, 2003, **2**, 739-743.
- 4 V. V. Vasisht, S. Saw, and S. Sastry, Liquid-liquid critical point in supercooled silicon, *Nature Phys.*, 2011, **7**, 549-553.
- 5 P. Ganesh and M. Widom, Liquid-Liquid Transition in Supercooled Silicon Determined by First-Principles Simulation, *Phys. Rev. Lett.*, 2009, **102**, 075701.
- 6 N. Jakse and A. Pasturel, Liquid-Liquid Phase Transformation in Silicon: Evidence from First-Principles Molecular Dynamics Simulations, *Phys. Rev. Lett.*, 2007, **99**, 205702.
- 7 D. T. Limmer and D. Chandler, The putative liquid-liquid transition is a liquid-solid transition in atomistic models of water, *J. Chem. Phys.*, 2011, **135**, 134503.
- 8 D. T. Limmer and D. Chandler, The putative liquid-liquid transition is a liquid-solid transition in atomistic models of water. II, *J. Chem. Phys.*, 2013, **138**, 214504.
- 9 J. C. Palmer, F. Martelli, Y. Liu, R. Car, A. Z. Panagiotopoulos, and P. G. Debenedetti, Metastable liquid-liquid transition in a molecular model of water, *Nature*, 2014, **510**, 385-388.
- 10 Y. Liu, J. C. Palmer, A. Z. Panagiotopoulos, and P. G. Debenedetti, Liquid-liquid transition in ST2 water, *J. Chem. Phys.*, 2012, **137**, 214505.
- 11 P. H. Poole, R. K. Bowles, I. Saika-Voivod, and F. Sciortino, Free energy surface of ST2 water near the liquid-liquid phase transition, *J. Chem. Phys.*, 2013, **138**, 034505.
- 12 J. Wedekind, R. Strey, and D. Reguera, New method to analyze simulations of activated processes, *J. Chem. Phys.*, 2007, **126**, 134103.

- 13 J. Wedekind and D. Reguera, Kinetic reconstruction of the free-energy landscape, *J. Phys. Chem. B*, 2008, **112**, 11060-11063.
- 14 S. E. M. Lundrigan and I. Saika-Voivod, Test of classical nucleation theory and mean first-passage time formalism on crystallization in the Lennard-Jones liquid, *J. Chem. Phys.*, 2009, **131**, 104503.
- 15 F. H. Stillinger and T. A. Weber, Computer simulation of local order in condensed phases of silicon, *Phys. Rev. B*, 1985, **31**, 5262-5271.
- 16 S. Nosé, A unified formulation of the constant temperature molecular dynamics methods, *J. Chem. Phys.*, 1984, **81**, 511-519.
- 17 W. G. Hoover, Canonical dynamics: Equilibrium phase-space distributions, *Phys. Rev. A*, 1985, **31**, 1695-1697.
- 18 W. Shinoda, M. Shiga and M. Mikami, Rapid estimation of elastic constants by molecular dynamics simulation under constant stress, *Phys. Rev. B*, 2004, **69**, 134103.
- 19 S. J. Plimpton, Fast parallel algorithms for short-range molecular dynamics, *J. Comp. Phys.*, 1995, **117**, 1-19.
- 20 D. Reguera, J. M. Rubi, and J. M. G. Vilar, The mesoscopic dynamics of thermodynamic systems, *J. Phys. Chem. B*, 2005, **109**, 21502-21515.
- 21 P. Hänggi, P. Talkner, and M. Borkovec, Reaction rate theory: Fifty years after Kramers, *Rev. Mod. Phys.*, 1990, **62**, 251-342.
- 22 E. Shiratani and M. Sasai, Molecular scale precursor of the liquid-liquid phase transition of water, *J. Chem. Phys.*, 1998, **108**, 3264-3276.
- 23 E. B. Moore, E. de la Llave, K. Welke, D. A. Scherlis, and V. Molinero, Freezing, melting and structure of ice in a hydrophilic nanopore, *Phys. Chem. Chem. Phys.*, 2010, **12**, 4124-4134.
- 24 A. C. Belch and S. A. Rice, The distribution of rings of hydrogen - bonded molecules in a model of liquid water, *J. Chem. Phys.*, 1987, **86**, 5676-5682.
- 25 M. Tanemura, T. Ogawa, and N. Ogita, A new algorithm for three-dimensional Voronoi tessellation, *J. Comp. Phys.*, 1983, **51**, 191-207.
- 26 L. O. Hedges, R. L. Jack, J. P. Garrahan, and D. Chandler, Dynamic order-disorder in atomic models of structural glass formers, *Science*, 2009, **323**, 1309-1313.
- 27 M. Avrami, Kinetics of phase change. I General theory, *J. Chem. Phys.*, 1939, **7**, 1103-1112.
- 28 L. Berthier and G. Biroli, Theoretical perspective on the glass transition and amorphous materials, *Rev. Mod. Phys.*, 2007, **83**, 587-645.
- 29 F. Smalenburg, L. Filion, and F. Sciortino, Erasing no-man's land by thermodynamically stabilizing the liquid-liquid transition in tetrahedral particles, *Nature Phys.*, 2014, **10**, 653-657.
- 30 I. Saika-Voivod, F. Smalenburg, and F. Sciortino, Understanding tetrahedral liquids through patchy colloids, *J. Chem. Phys.*, 2013, **139**, 234901.
- 31 F. Smalenburg and F. Sciortino, Tuning the liquid-liquid transition by modulating the hydrogen-bond angular flexibility in a model for water, *Phys. Rev. Lett.*, 2015, **115**, 015701.
- 32 T. Yagasaki, M. Matsumoto, and H. Tanaka, Spontaneous liquid-liquid phase separation of water, *Phys. Rev. E*, 2014, **89**, 020301(R).
- 33 E. B. Moore and V. Molinero, Ice crystallization in water's "no-man's land", *J. Chem. Phys.*, 2010, **132**, 244504.
- 34 I. Kohl, E. Mayer, and A. Hallbrucker, The glassy water-cubic ice system: a comparative study by X-ray diffraction and differential scanning calorimetry, *Phys. Chem. Chem. Phys.*, 2000, **2**, 1579-1586.
- 35 S. Sastry, P. G. Debenedetti, F. Sciortino, and H. E. Stanley, Singularity-free interpretation of the thermodynamics of supercooled water, *Phys. Rev. E*, 1996, **53**, 6144-6154.
- 36 K. Zhang, H. Li, and Y. Y. Jiang, Liquid-liquid phase transition in quasi-two-dimensional supercooled silicon, *Phys. Chem. Chem. Phys.*, 2014, **16**, 18023.
- 37 C. Desgranges and J. Delhommelle, Role of liquid polymorphism during the crystallization of silicon, *J. Am. Chem. Soc.*, 2011, **133**, 2872-2874.
- 38 A. Hedler, S. L. Klaumünzer, and W. Wesch, Amorphous silicon exhibits a glass transition, *Nature Mater.*, 2004, **3**, 804-809.
- 39 P. Beaucage and N. Mousseau, Liquid-liquid phase transition in Stillinger-Weber silicon, *J. Phys.: Condens. Matter*, 2005, **17**, 2269-2279.